# MATERIAL REMOVAL AND TOOL WEAR ANALYSIS BY ECDM DRILLING OF A MOSAIC CERAMIC MATERIAL

**Pravin Pawar[1], Raj Ballav[2], Amaresh Kumar[3]**

[1,2,3] Manufacturing Engineering Department, National Institute of Technology (N.I.T.), Jamshedpur, Jharkhand, 831014, India

Corresponding author: Pravin Pawar, pravin.1900@gmail.com

***Abstract:*** The Electrochemical Discharge Machining (ECDM) is a combined machining process which has applicable for the machining of high strength non-conducting materials having high hardness. In present investigation the drilling process of ECDM is applied on (Mosaic) ceramic material. The experiments were intended with reference to the Taguchi $L_{27}$ orthogonal array and scrutinized through MINITAB 17 software. For the assessment of tool wear rate (TWR) and material removal rate (MRR) the input factors taken for investigational studies as voltage, rotation speed of tool electrode and electrolyte concentration. Thus, according to the observed results it can be concluded that the most dominant parameter for MRR and TWR is voltage followed by electrolyte concentration and rotation.

***Key words:*** Electrochemical Discharge Machining, Mosaic ceramic, material removal rate, tool wear rate.

## 1. INTRODUCTION

The manufacturing process is executed to make changes in shape, dimensions and surface finish to obtain a high-quality product. A newly industrialized process i.e combined traditional and non-traditional machining is utilized to machine the ceramic and composite material which exhibits characteristics like high hardness and brittleness, [1]. In this process forming or deformation of materials occurs because of the effect of energy in a range of variations i.e. laser processing (utilizing the energy of photons) , ion beam machining (applying the energy of the ions), electrical discharge machining (applying the electric discharges), plasma beam machining (producing the effect of thermal energy), [2]. The drilling operation is mostly applied in the machining process. Though, thermal cutting significance is a basic characteristic in drilling operation, [3]. The finite element model is used to analyze, simulate and predict drilling cutting results from input process parameters, [4]. The electrochemical discharge machining is amalgam of two manufacturing process which is electro-chemical machining (ECM) and electro-discharge machining (EDM) process. The material removal is done by two ways viz thermal removal of material due to electrical discharges and electrochemical dissolution of the material which was observed between electrodes i.e anode and cathode, [5]. The electrochemical discharge machining process (ECDM) is mostly used for micro drilling and micro channel machining process in conducting and non-conducting materials. This process as well recognized as sparks assisted chemical engraving and electrochemical spark machining, [6]. Kurafuji et al. invented firstly ECDM process applied for drilling on glass material in year 1968, [7]. Wuthrich et al. reveals that the machining with electrochemical discharge phenomena is occurred only above the critical voltage i.e. in the arc region, [8]. Pawar et al. reveals that the many researchers applied NaOH as electrolyte, Tungsten carbide as cathode and Graphite as anode material, [9]. Jain et al. [10] and Chak et al., [11] observed increased material removal rate (MRR), cutting and machining ability in ECDM process which is an effect of abrasive tool electrode. Coteata et al., [12] obtained small diameter holes in steel material by slotter ram mechanism with electrochemical discharge machine. Similarly, Huang et al. [13] drilled micro hole on stainless steel material by high-speed rotation tool electrode in ECDM. In present study, the MRR and tool wear rate (TWR) were examined by using ECDM drilling process which is applied on Mosaic ceramic material and the brass is taken as cathode tool material.

## 2. BASIC WORKING PRINCIPLE OF ECDM

In this process, the electrolytically heat gets generated due to accelerated chemical reaction and electrical discharge. The chemical reaction between the workpiece surface and electrolyte is obtained by heat which is resulted into removal of the workpiece surface. Figure 1 represents a schematic depiction of ECDM machining process. The anode tool and cathode tool electrode is dipped in ECDM rectangular electrolyte container and D.C. power supply connected between them. When D.C. voltage is applied, hydrogen bubbles produced on cathode tool and oxygen bubbles produced on anode tool electrode. Then after increasing more voltage the high intensity hydrogen bubbles get generated. Consequently, the bubbles developed dense and coalesced which creates a gas film on the cathode tool electrode. After, increasing more voltage the breaking of gas film take place and the high intensity flow of electrons from cathode to electrolyte produces spark, [14].

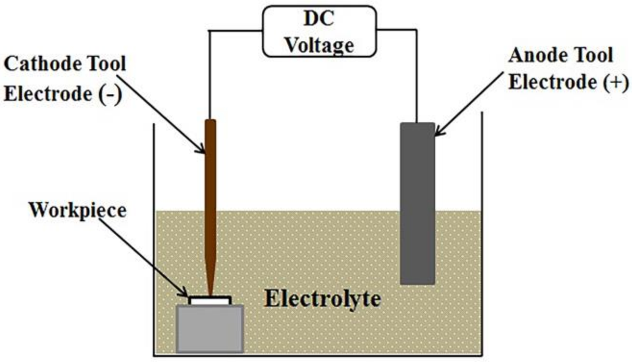


Fig. 1. Basic Schematic Diagram of ECDM

## 3. EXPERIMENTAL SETUP

The schematic diagram and fabricated ECDM setup are presented in Figure 2 and Figure 3. The X-Y movement of the workpiece is controlled by a compound slide which is fixed on the table and workpiece which is stable on holding fixture which is placed in the ECDM electrolyte cell. The cathode tool is attached to the Z axis and the movement of the tool is controlled by a single axis compound slide manually. The gravity feeding mechanism is applied to the workpiece during ECDM machining process.
The speed of stepper motor attached with cathode tool is monitored by Arduino Uno board from the computer. In between cathode and anode tool electrode DC voltage is provided. For cathode tool electrode brass of 3mm diameter is taken. Whereas for anode electrode the stainless steel 416 of 15mm diameter is used. Both the electrods are placed into a NaOH electrolyte container. The machining time is set to be 25 min for each experiment. Figure 4 shows that sparking during ECDM drilling on Mosaic Ceramic.

## 4. EXPERIMENTAL METHODOLOGY AND PROCESS PARAMETERS

The micro hole is drilled on 150×125×8mm$^3$ Mosaic ceramic plate by using ECDM process. The drilling of mosaic ceramic experiments was investigated by using Taguchi $L_{27}$ orthogonal array method.

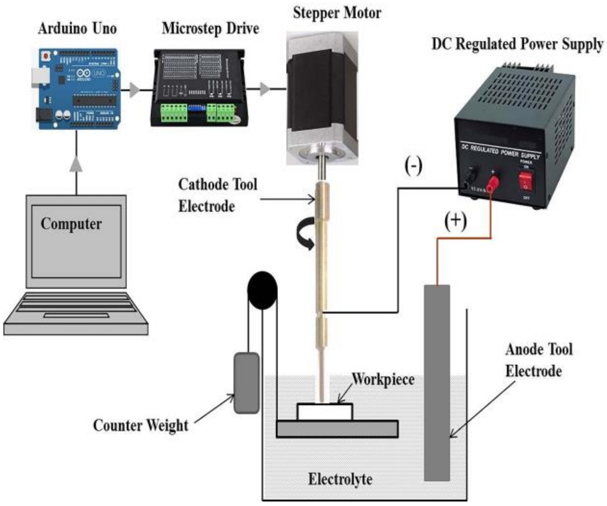


Fig. 2. Schematic Diagram of ECDM setup

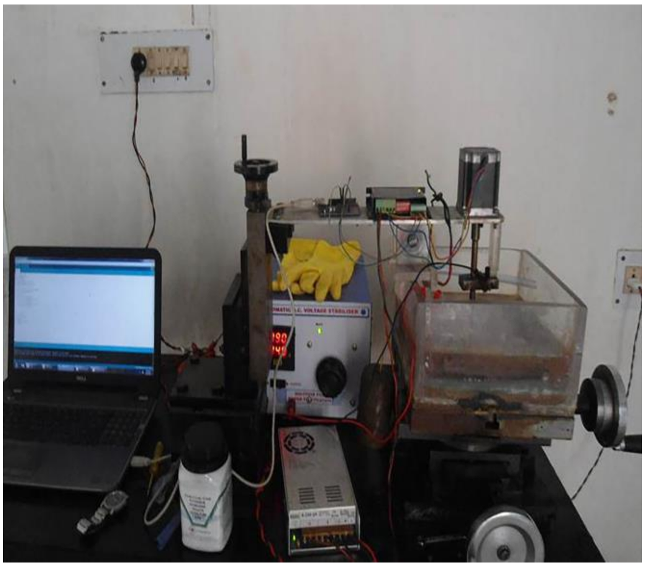

Fig. 3 Fabricated ECDM Setup

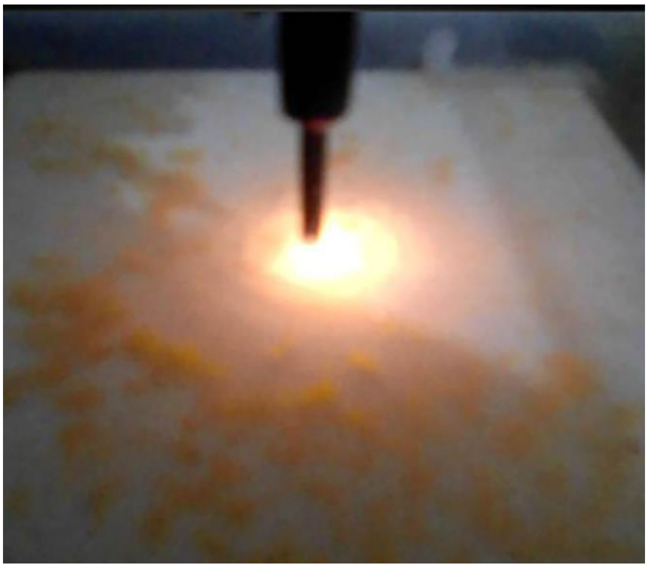

Fig. 4. Sparking during ECDM drilling on Mosaic Ceramic

Table 1 represents three factors and their three levels that significance to construct either $L_9$ with multiple replication or $L_{27}$ OA, where 9 and 27 denotes the number of trials and L shows the level of the trials. On the bases of total degree of freedom essential for an experiment the $L_{27}$ orthogonal array was preferred. In the present work selecting three factors with three levels and their two-way interactions taking into consideration therefore the total degree of freedom is 18. In view of that, $L_{27}$ orthogonal array was decided for current research work which has 26 degrees of freedom. The voltage, electrolyte concentration and rotation are taken as input machining parameters. While, the MRR and TWR are considered as output responses, [15].

Table 1. Important Process Parameters and Their Levels

| Factor | Parameters | Unit | Levels | | |
|---|---|---|---|---|---|
| | | | 1 | 2 | 3 |
| A | Voltage | V | 70 | 80 | 90 |
| B | Rotation speed | rpm | 10 | 25 | 40 |
| C | Electrolyte Concentration | % | 5 | 10 | 15 |

The MRR and TWR were observed with the help of precision weight machine. The following formulas (1) and (2) given by Pawar et al. and Paul et al. [16, 17] are used to calculate the MRR and TWR.

$$MRR = \frac{(Iw)_w - (Fw)_w}{t} \quad (1)$$

$$TWR = \frac{(Iw)_T - (Fw)_T}{t} \quad (2)$$

where, $(Iw)_w$ = initial weight of workpiece, mg; $(Fw)_w$= final weight of workpiece, mg; $(Iw)_T$ = initial weight of tool, mg; $(Fw)_T$ = final weight of tool, mg; t = machining time, min.

The experimental results are presented in Table 2 which emphasizes the input process parameter, output responses and the SN ratios. SN ratios exhibit the higher value which signifies better machining performance such as MRR at higher the better while, lower the better for TWR. The S/N ratio is evoked from experimental data by using Minitab 17 software. The S/N ratio gives measures of robustness to identify the control factors that reduce the variability of the process. The S/N ratio is evaluated by utilizing the following formula (3), [17].

$$S/N = -10\log\left(\frac{1}{n}\sum_{i=1}^{n}\frac{1}{y_i^2}\right) \quad (3)$$

where n represents the number of measurements and $y_i$ is the measured values.

Table 2. Experimental results and signal-to-noise ratio

| Run | Voltage (V) | Rotation speed (rpm) | Electrolyte concentration (%) | MRR (mg/min) | TWR (mg/min) | S/N ratios MRR (dB) | S/N ratios TWR (dB) |
|---|---|---|---|---|---|---|---|
| 1 | 70 | 10 | 5 | 0.122 | 0.024 | -18.2728 | 32.3958 |
| 2 | 70 | 10 | 10 | 0.151 | 0.054 | -16.4205 | 25.3521 |
| 3 | 70 | 10 | 15 | 0.233 | 0.076 | -12.6529 | 22.3837 |
| 4 | 70 | 25 | 5 | 0.134 | 0.021 | -17.4579 | 33.5556 |
| 5 | 70 | 25 | 10 | 0.164 | 0.058 | -15.7031 | 24.7314 |
| 6 | 70 | 25 | 15 | 0.263 | 0.078 | -11.6009 | 22.1581 |
| 7 | 70 | 40 | 5 | 0.138 | 0.028 | -17.2024 | 31.0568 |
| 8 | 70 | 40 | 10 | 0.176 | 0.061 | -15.0897 | 24.2934 |
| 9 | 70 | 40 | 15 | 0.256 | 0.084 | -11.8352 | 21.5144 |
| 10 | 80 | 10 | 5 | 0.484 | 0.085 | -6.3031 | 21.4116 |
| 11 | 80 | 10 | 10 | 0.678 | 0.132 | -3.3754 | 17.5885 |
| 12 | 80 | 10 | 15 | 0.834 | 0.280 | -1.5767 | 11.0568 |
| 13 | 80 | 25 | 5 | 0.476 | 0.091 | -6.4479 | 20.8192 |
| 14 | 80 | 25 | 10 | 0.710 | 0.143 | -2.9748 | 16.8933 |
| 15 | 80 | 25 | 15 | 0.865 | 0.271 | -1.2597 | 11.3406 |
| 16 | 80 | 40 | 5 | 0.497 | 0.084 | -6.0729 | 21.5144 |
| 17 | 80 | 40 | 10 | 0.725 | 0.152 | -2.7932 | 16.3631 |
| 18 | 80 | 40 | 15 | 0.915 | 0.288 | -0.7716 | 10.8122 |
| 19 | 90 | 10 | 5 | 0.640 | 0.296 | -3.8764 | 10.5742 |
| 20 | 90 | 10 | 10 | 0.982 | 0.480 | -0.1578 | 6.3752 |
| 21 | 90 | 10 | 15 | 1.120 | 0.683 | 0.9844 | 3.2989 |
| 22 | 90 | 25 | 5 | 0.694 | 0.312 | -3.1728 | 10.1169 |
| 23 | 90 | 25 | 10 | 1.120 | 0.511 | 0.9844 | 5.7807 |
| 24 | 90 | 25 | 15 | 1.230 | 0.715 | 1.7981 | 2.9260 |

| | | | | | | | |
|---|---|---|---|---|---|---|---|
| 25 | 90 | 40 | 5 | 0.715 | 0.320 | -2.9139 | 9.8970 |
| 26 | 90 | 40 | 10 | 1.154 | 0.567 | 1.2441 | 4.9283 |
| 27 | 90 | 40 | 15 | 1.320 | 0.748 | 2.4115 | 2.5220 |

## 5. RESULTS AND DISCUSSION

The analysis is conducted by using MINITAB 17 software. A Taguchi approach significantly improves the engineering processes as it decreases time required and cost involved in trials. Attainment of parameters in Taguchi approach is verified by signal to noise ratio (S/N) [18].

### 5.1 Effect on MRR

The MRR increases with increase in voltage. The observation shows that in the voltage range from 70V to 90V MRR observed to be increased. Hence, owing to increase in voltage, the rate of gas bubbles formation gets increases which indicate a larger amount of discharge energy in the sparking zone. Also, the increased MRR was observed due to the percentage of electrolyte concentration resulted into increased amount of current, which accelerates the electrolysis process resulting into high intensity hydrogen gas bubbles occurs at the cathode, [19, 20]. The experimental results and XRD pattern of mosaic ceramic material is shown in Fig. 5 and Fig. 6.

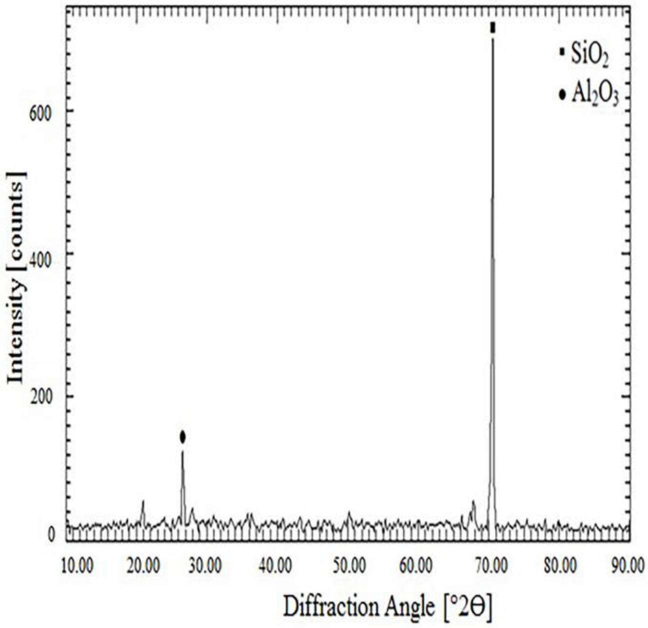


Fig. 6. XRD pattern of Mosaic ceramic tile

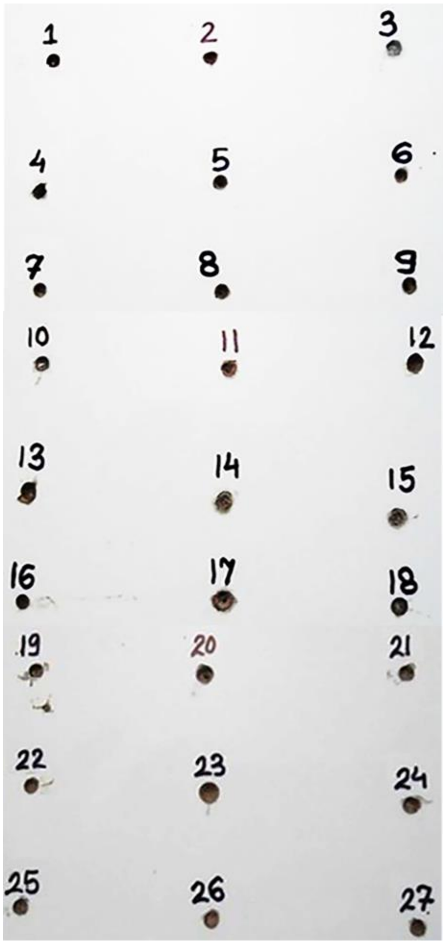


Fig. 5. Experimental Results after ECDM Drilling

The mean S/N ratios plot for MRR is given in Figure 7. It represents an effect of each parameter on MRR. According to it the voltage is the most significant parameter because as it increases the MRR also increases. The surface plots of MRR vs. influencing input parameters i.e. voltage, electrolyte concentration and rotation is shown in Fig. 8 and Fig. 9.

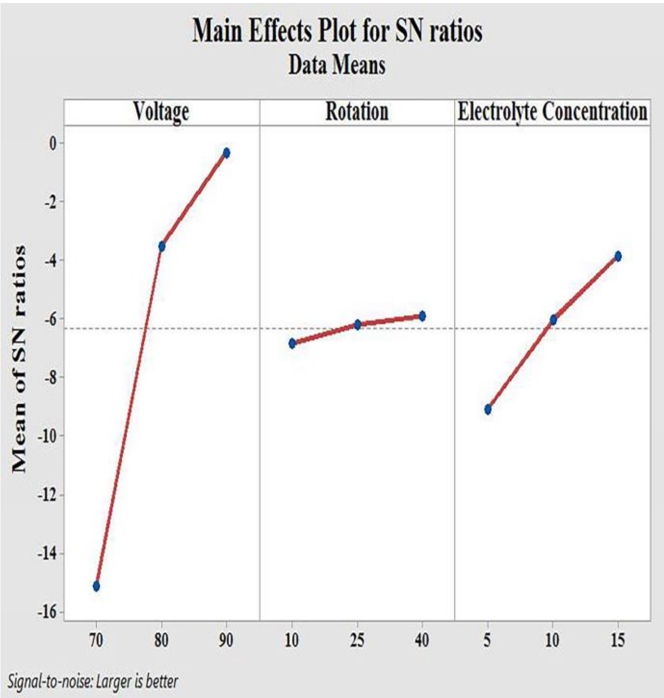


Fig. 7. Mean S/N ratios plot for MRR

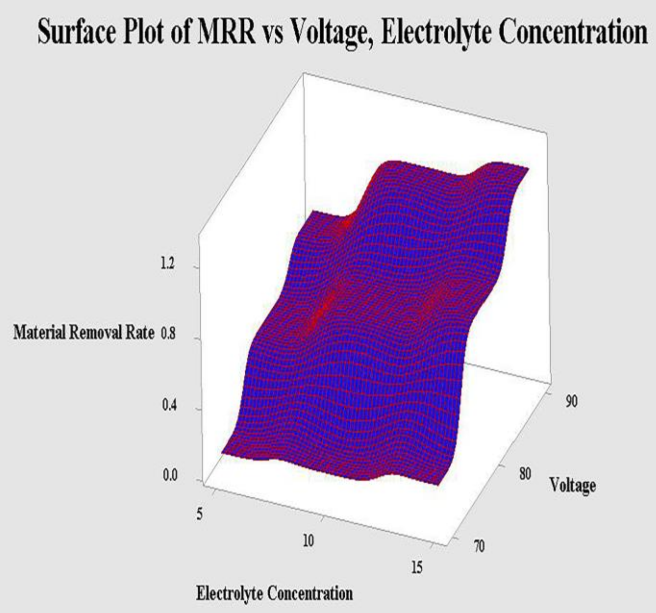


Fig. 8. Surface plot of MRR vs Voltage, Electrolyte concentration

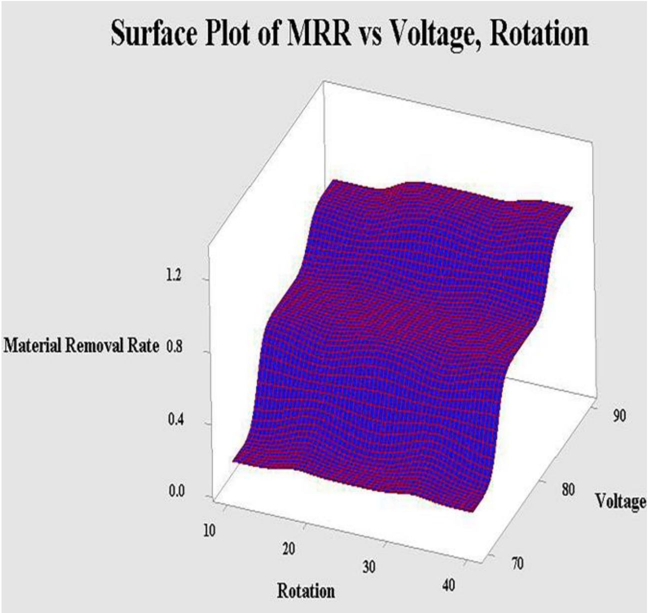


Fig. 9. Surface plot of MRR vs Voltage, Rotation

To scrutinize the influence of individual process parameters the ANOVA is utilized. The delta value denotes the difference in maximum and minimum average value of S/N ratios of each process parameters. The optimal level of parameters chosen based on higher values in S/N table. The larger F-value designates a significant change on output response affected owing to variation in process parameters. An ANOVA test was done to validate the goodness of fit of the developed mathematical model. The table 3 shows response individual average for each level of per factor. The table states the ranks based on delta measurements. Although, the Minitab 17 allocates ranks be contingent on delta values i.e. rank 1 for topmost delta value then rank 2 for next uppermost and so on. The ranks designate the significance of each factor in the response. The ranks and delta values denoted that voltage has the greatest effect on MRR which is followed by electrolyte concentration and rotation. A mathematical model for MRR is investigated through MINITAB 17 software which is specified in eq. (4). The ANOVA for MRR is given in table 4. The values of p indicate that the differences between F are statistically significant.

MRR = -3.048 + 0.04077 Voltage + 0.03484 Electrolyte Concentration + 0.00241 Rotation (4)

Table 3. Response Table for S/N Ratios of Material removal rate

| Level | Voltage (V) | Electrolyte Concentration (%) | Rotation |
|---|---|---|---|
| 1 | -15.1373 | -9.0800 | -6.8501 |
| 2 | -3.5084 | -6.0318 | -6.2038 |
| 3 | -0.2998 | -3.8337 | -5.8915 |
| Delta | 14.8374 | 5.2463 | 0.9586 |
| Rank | 1 | 2 | 3 |

Table 4. ANOVA Table for Material Removal Rate

| Source | DF | Adj SS | Adj MS | F-Value | P-Value |
|---|---|---|---|---|---|
| Voltage | 2 | 3.0485 | 1.5242 | 166.0 | 0.000 |
| Electrolyte Concentration | 2 | 0.5577 | 0.2788 | 30.38 | 0.000 |
| Rotation | 2 | 0.0241 | 0.0120 | 1.32 | 0.290 |
| Error | 20 | 0.1835 | 0.0091 | | |
| Total | 26 | 3.8140 | | | |
| S | R-sq | | R-sq(adj) | R-sq(pred) | |
| 0.0958079 | 95.19% | | 93.74% | 91.23% | |

### 5.2 Effect on TWR

The voltage has the greatest influence on the TWR, followed by the electrolyte concentration and rotation. The TWR enhanced from 0.024 mg/min up to 0.748 mg/min with enhanced voltage from 70V up to 90V [13, 22]. The increased TWR resulted into diminishing of electrode tool diameter of applied voltage and electrolyte concentration [23]. The tool electrode erosion influenced by on various aspects such as applied voltage, capacity of the relaxation circuits, workpiece and electrode tool materials properties, tool electrode velocity, type and properties of electrolyte solution etc., [24]. The figure 10 shows the cathode tool electrode before machining and after machining. Figure 11 shows XRD pattern of brass tool electrode.


Fig. 10. Cathode tool wear: (a) Before machining, (b) After machining

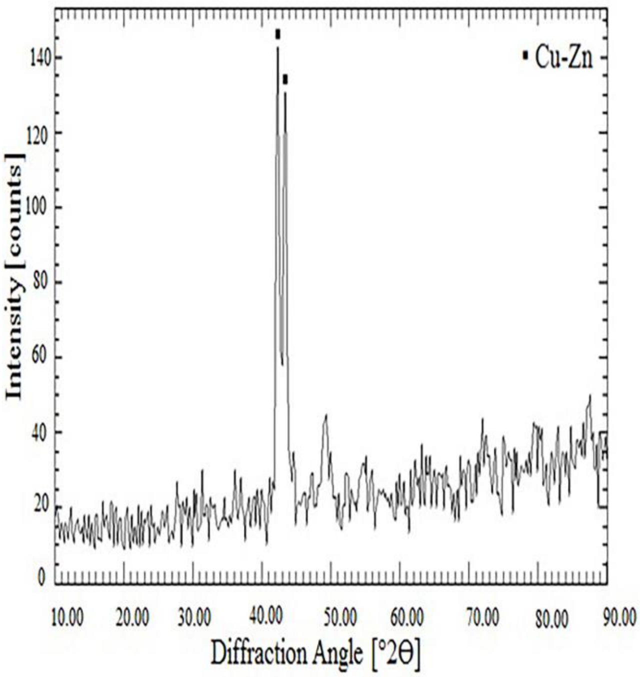


Fig. 11. XRD pattern of brass cathode tool

The plot of TWR mean S/N ratios specifies the effect of each parameter on TWR shown in Fig.12 which presents the effect of voltage, electrolyte concentration and rotation on TWR. According to this figure the increase in voltage ensuing increase in TWR hence, it is the most significant parameter. The surface plots of TWR vs. influencing input parameters i.e. voltage, electrolyte concentration and rotation is shown in Figure 13 and 14.

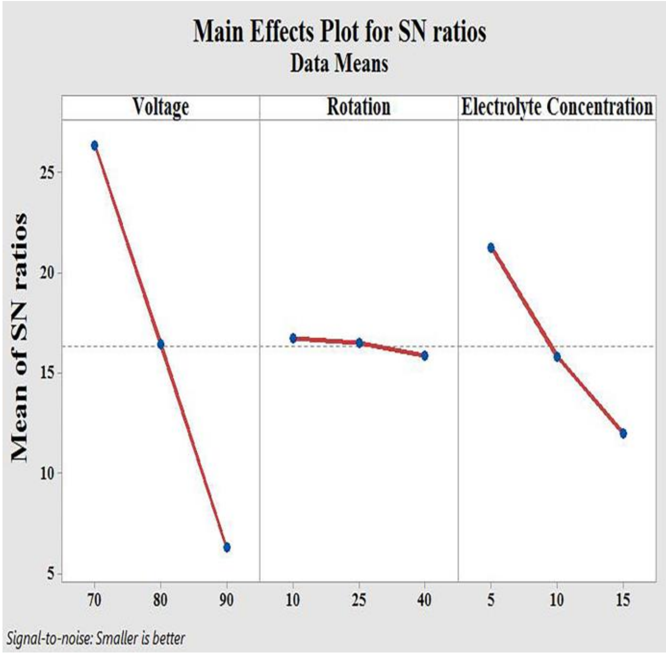


Fig. 12. Mean S/N ratios plot for Tool Wear Rate

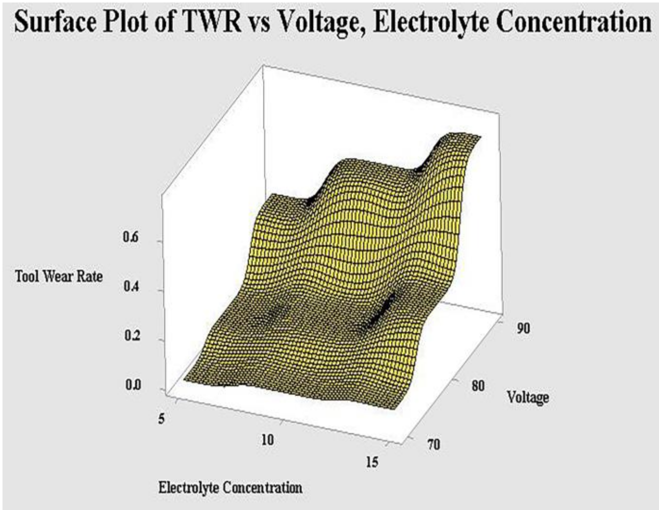


Fig. 13. Surface plot of TWR vs Voltage, Electrolyte concentration

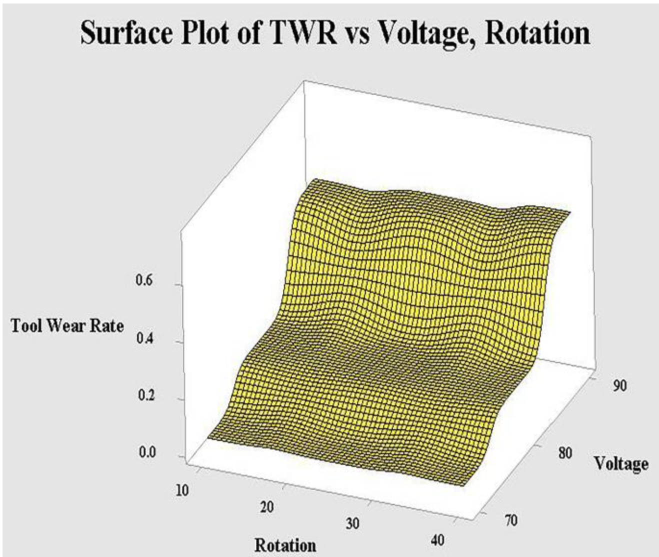


Fig. 14. Surface plot of TWR vs Voltage, Rotation

The response table 5 depicts the response characteristic average for each level of per factor. According to the values of ranks and delta the voltage is most affecting parameter on TWR followed by electrolyte concentration and rotation. The analysis of variance (ANOVA) for TWR is given in table 6. It shows that the voltage and electrolyte concentration are the most significant parameters followed by rotation (Delta – table 5 and F – table 6). The equation (5) shows mathematical model for the tool wear rate developed by using MINITAB 17 software.

$$TWR = -1.837 + 0.02306\ Voltage + 0.02180\ Electrolyte\ Concentration + 0.00082\ Rotation \quad (5)$$

Table 5. Response Table for S/N Ratios of Tool wear rate

| Level | Voltage | Electrolyte Concentration | Rotation |
|---|---|---|---|
| 1 | 26.382 | 21.260 | 16.715 |
| 2 | 16.422 | 15.812 | 16.480 |
| 3 | 6.269 | 12.001 | 15.878 |
| Delta | 18.70 | 9.259 | 0.837 |
| Rank | 1 | 2 | 3 |

Table 6. ANOVA Table for Tool wear rate

| Source | DF | Adj SS | Adj MS | F-Value | P-Value |
|---|---|---|---|---|---|
| Voltage | 2 | 1.0363 | 0.5181 | 102.8 | 0.000 |
| Electrolyte Concentration | 2 | 0.2143 | 0.1071 | 21.27 | 0.000 |
| Rotation | 2 | 0.0027 | 0.0013 | 0.27 | 0.765 |
| Error | 20 | 0.1007 | 0.0050 | | |
| Total | 26 | 1.3542 | | | |

| S | R-sq | R-sq(adj) | R-sq(pred) |
|---|---|---|---|
| 0.0709797 | 92.56% | 90.33% | 86.44% |

## 6. CONCLUSIONS

The ECDM setup is build and fabricated for machining of non-conducting materials. In this work, two output responses are investigated i.e. MRR and TWR on the bases of three input process parameters i.e. voltage, rotation and electrolyte concentration. The experimental work was carried out on Mosaic ceramic material with using Brass as cathode electrode in ECDM. On the bases of Taguchi $L_{27}$ Orthogonal Array method the design of experiments were carried out. Thus from this study it can be concluded that for MRR the voltage is the most significant parameter followed by electrolyte concentration. Similarly, for TWR the voltage and electrolyte concentration are the most significant parameters. Hence, the higher values of voltage and electrolyte concentration are produces higher MRR. While, the lower values of voltage and electrolyte concentration resulted into lower TWR.


**ACKNOWLEDGEMENTS**

The authors would like to acknowledge Manufacturing Engineering Deparment for providing essential facilities and the Metallurgy Engineering Department of, National Institute of Technology (N.I.T.), Jamshedpur for providing lab facilities for XRD analysis of the materials.


## 7. REFERENCES


1. Pawar, P., Ballav, R., Kumar, A., (2017). *Machining Processes of Sapphire: An Overview*, International Journal of Modern Manufacturing Technologies, 9(1), 47-72.
2. Gherman, L., Palaghia, I., Dodun, O., Slatineanu, L., (2012). *Statistic Analysis of The Experimental Results Obtained At Single Discharge Electroerosion*, International Journal of Modern Manufacturing Technologies, 4(2), 39-46.
3. Mourad, A., Mourad, B., Abderrahim, B., Gheorghe, B., (2016). *Numerical Study of Cutting Temperature During Drilling Process of The C45 Steel*, International Journal of Modern Manufacturing Technologies, 8(2), 42-47.
4. Pawar, P., Ballav, R., Kumar, A., (2016). *Finite Element Method Broach Tool Drilling Analysis Using Explicit Dynamics Ansys*, International Journal of Modern Manufacturing Technologies, 8(2), 54-60.
5. Pawar, P., Ballav, R., Kumar, A. (2015). *Measurement Analysis in Electrochemical Discharge Machining (ECDM) Process: A Literature Review*, J. Chem. Chem. Eng., 9, 140-144.
6. Pawar, P., Ballav, R., Kumar, A., (2017). *Recent status of Spark Assisted Chemical Engaving: A Review*, Journal of Chemical and Pharmaceutical Sciences, 10(2), 1015-1020.
7. Kurafuji, H., Suda, K., (1968). *Electrical discharge drilling of glass*, Annals of the CIRP, 16, 415–419.
8. Wuthrich, R., Fascio, V., (2005). *Machining of non-conducting materials using electrochemical discharge phenomenon-an overview*, International Journal of Machine Tools and Manufacture, 45, 1095–1108.
9. Pawar, P., Ballav, R., Kumar, A., (2015). *Revolutionary Developments in ECDM Process: An Overview*, Materials Today: Proceedings, 2, 3188-3195.
10. Jain, V.K., Choudhury, S.K., Ramesh, K.M. (2002). *On the machining of alumina and glass*, International Journal of Machine Tools and Manufacture, 42, 1269–1276.

11. Chak, S.K., Rao, P.V., (2008). *The drilling of $Al_2O_3$ using a pulsed DC supply with a rotary abrasive electrode by the electrochemical discharge process*, The International Journal of Advanced Manufacturing Technology, 39, 633–641.
12. Coteata, M., Schulze, H.P., Slatineanu, L., (2011). *Drilling of Difficult-to-Cut Steel by Electrochemical Discharge Machining*, Materials and Manufacturing Processes, 26, 1466–1472.
13. Huang, S.F., Liu, Y., Li, J., Hu, H.X., Sun, L.Y., (2014). *Electrochemical Discharge Machining Micro-Hole in Stainless Steel with Tool Electrode High-Speed Rotating*, Materials and Manufacturing Processes, 29, 634–637.
14. Pawar, P., Sinha, S., Kumar, A., Ballav, R., (2014). *Review on Research Trends in Electrochemical Discharge Machining*, 4$^{th}$ National Conference on Recent in Advances in Manufacturing (RAM-2014), India. 132-136.
15. Coskun, S., Motorcu, A.R., Yamankaradeniz, N., Pulat, E., (2012). *Evaluation of control parameters' effects on system performance with Taguchi method in waste heat recovery application using mechanical heat pump*, International Journal of Refrigeration, 35, 795-809.
16. Pawar, P., Anasane, S., Ballav, R., Kumar, A. (2016). *Experimental Study of Electroless Copper Coated On ABS Material Used For Tooling In EDM Machining Process*, Journal of Production Engineering, 19(2), 27-32.
17. Paul, L., Hiremath, S.S., (2013). *Response Surface Modelling of Micro Holes in Electrochemical Discharge Machining Process*, Procedia Engineering, 64, 1395–1404.
18. Powar, P.P., Raval, H.K, (2016). *A Study On Process Parameters Effect In Hard Turning of En24 Steel Using Minimum Quantity Lubrication (MQL)*, International Journal of Modern Manufacturing Technologies, 8(2), 66-71.
19. Paul, L., Hiremath, S.S., (2014). *Characterisation of Micro Channels in Electrochemical Discharge Machining Process*, Applied Mechanics and Materials, 490-491, 238-242.
20. Sarkar, B., Doloi, B., Bhattacharya, B., (2006). *Parametric analysis on electrochemical discharge machining of silicon nitride ceramics*, International Journal of Advanced Manufacturing Technology, 28(9), 873-881.
21. Roy, A., Nath, N., Nedelcu, D., (2017). *Experimental Investigation on Variation of Output Responses of As Cast TiNiCu Shape Memory Alloys Using Wire EDM*, International Journal of Modern Manufacturing Technologies, 9(1), 90-101.
22. Madhavi, B., Hiremat, S.S., (2016). *Investigation on Machining of Holes and Channels on Borosilicate and Sodalime Glass using u-ECDM Setup*, Procedia Technology, 25, 1257–1264.
23. Coteata, M., Slatineanu, L., Dodun, O., Ciofu, C. (2008). *Electrochemical discharge machining of small diameter holes*, International Journal of Material Forming, 1, 1327–1330.
24. Coteaţa, M., Ciofu, C., Slatineanu, L., Munteanu, A., Dodun, O., (2009). *Establishing the Electrical Discharges Weight In Electrochemical Discharge Drilling*, International Journal of Material Forming, 2(1), 673–676.

Received: July 8, 2017 / Accepted: December 10, 2017 / Paper available online: December 20, 2017 